Korean J. Chem. Eng., 32(5), 882-895 (2015)
DOI: 10.1007/s11814-014-0308-8

pISSN: 0256-1115
eISSN: 1975-7220

Efficient removal of crystal violet and eosin B from aqueous solution using *Syzygium cumini* leaves: A comparative study of acidic and basic dyes on a single adsorbent

Arshad Mehmood*,†, Sheher Bano*, Aisha Fahim, Riffat Parveen*, and Shazia Khurshid***

*Department of Chemistry, GC University Lahore, Lahore 54000, Pakistan
**Department of Chemistry, The Government Sadiq College Women University Bahawalpur, Pakistan
(*Received 24 March 2014 • accepted 9 October 2014*)

Abstract−The adsorption capabilities of *Syzygium cumini* leaves were investigated for crystal violet and eosin B using batch adsorption method. Removal conditions were optimized by varying operational parameters like pH, dose of adsorbent, contact time and temperature. Presence of salts had a profound effect on the adsorption and the experimental data for both adsorbates, providing good correlation with the Temkin, Langmuir and Freundlich patterns, but differing from Dubinin-Radushkevich model. Maximum adsorption capacity was found to be 38.75 mg/g for crystal violet and 16.28 mg/g for eosin B respectively. Boyd-Adamson-Myers, Morris-Weber and Bangham's surface mass transport models revealed that film diffusion was the rate controlling process and followed pseudo-second order kinetics. Activation energy was estimated to be 57.265 and 6.721 kJ/mol for crystal violet and eosin B respectively. Adsorption of crystal violet is endothermic and that of Eosin B is exothermic but both were spontaneous at all temperatures. To study the bulk removal of the dyes, column operations were made. The exhausted columns were regenerated by eluting HCl solution and almost 91.94% of CV and 58.08% of EB were recovered from columns, respectively.

Keywords: Dyes, Crystal Violet, Eosin B, Adsorption, *Syzygium cumini*, Surface Mass Transport

INTRODUCTION

The unconsumed dyes from different industrial units, like textile, paint, acrylic, cosmetics, plastics, paper and pulp, Kraft bleaching, tanning, and pharmaceutical are released into water bodies and are considered as organic pollutants [1]. Among 7×10^5 tons annually produced dye stuff [2], 12% are lost during manufacturing and processing operations, 30% are used in textile industry [1,3], which directly discharge around 2-20% in aqueous effluents into hydrosphere, and 10-25% are lost during the dyeing process [4]. Discharging of dye-containing effluents into hydrosphere is prohibited not only because of their color, which reduces the sunlight penetration into the water, but also because of toxic, carcinogenic and mutagenic nature of their breakdown products [5]. If adequate removal methods are not used, most of these dyes remain in the aquatic system for a longer span of time, sometimes more than 40 years [6], even discoloration of dye containing waste water cannot be attained when treated aerobically using municipal sewerage systems [7].

A variety of techniques have been reported for the treatment of dye-contaminated industrial effluents, which include membrane filtration, ion-exchange membranes, electrochemical degradation, integrated chemical/biological degradation, integrated iron (III) photo-assisted biological treatment, solar photo-Fenton and biological processes, coagulation, chemical precipitation, solvent extraction, reverse osmosis, photocatalytic degradation, sonochemical degradation and micellar enhanced ultrafiltration [8]. Above all, adsorption has proved itself a state of the art technique due to its certain salient features like insensitivity to toxic pollutants, high efficiency, low cost, operational ease and flexibility. A large variety of materials, both natural and synthetic, have been used as adsorbent for the removal of dyes from aqueous medium but those based on biological materials like biomass, agricultural solid wastes and plant products are often much more selective, competitive, effective and cheaper than traditional synthetic materials like ion-exchange resins and commercial activated carbons, and can reduce the dye concentration to ppb levels [8]. Low cost biological adsorbent or bioadsorbents like banana peels [9], rice straw [10], orange peels [11], alga sargassum muticum seaweed [12], dead macro fungi [13], hydrilla verticillata [14], moss [15], saw dust [16] and hundreds of others have been reported to remove pollutants from water, but search for ideality regarding availability, efficiency and low cost is still there.

Any dye can be classified as cationic, nonionic or anionic type depending on its structure and properties [3]. Anionic dyes, which are also called acidic dyes or reactive dyes [17], are most problematic in water treatment because they pass through conventional treatment systems unaffected [18]. Cationic dyes are basic dyes having intense color and extensively used to impart bright shades to textile products. The present work investigates the comparative adsorption behavior of crystal violet (CV) which is a basic dye and eosin B (EB) an acidic dye, on a cheap, largely available and low cost adsorbent obtained from the leaves of *Syzygium cumini*. The operational parameters like initial solution pH, the dose of adsor-

†To whom correspondence should be addressed.
E-mail: arshadmehmood@gcu.edu.pk

Table 1. Elemental analysis and surface area characterization of adsorbent

Element analysis of adsorbent					
Element	C	H	N	S	O
% Age	41.51±0.50	6.97±0.50	1.06±0.50	0.87±0.20	13.84±0.50
Surface area and pore size analysis					
BET surface area ($m^2 g^{-1}$)		Langmuir surface area ($m^2 g^{-1}$)		Pore volume ($cm^3 g^{-1}$)	Pore diameter (Å)
5.98		38.16		0.07	121.96

bent, contact time, ionic strength and temperature have been optimized using batch adsorption method. Adsorption kinetics, isothermal models, thermodynamics parameters and adsorption mechanism were evaluated comprehensively and are reported. The potential of adsorbent for aqueous removal of dyes was further tested in a fixed-bed continuous flow column using self-made wastewater. Column regeneration and recycling was also carried out to consider its industrial applicability for bulk removal of the both CV and EB. The study is unique as there is no existing report for the removal of any dye by *Syzygium cumini*.

EXPERIMENTAL

1. Reagents

All the reagents, used in the present work, were of analytical grade and procured from E. Merck, Germany. Crystal violet (CV) and eosin B (EB) with 99.9% purity, used as adsorbate were not further purified prior to use. Physicochemical characteristics of these dyes are given in Table 1. Stock solutions of both dyes (1,000 mg L^{-1}) were prepared by dissolving accurately weighed quantity of the dye in distilled water. Solutions of different concentrations used in the further experiments were prepared by diluting the stock solution with suitable volume of distilled water. The initial pH of the solution was adjusted using 0.1 M HCl and 0.1 M NaOH solutions. Throughout the experiments, glassware used was washed with chromic acid and then repeatedly washed with distilled water, followed by drying at room temperature for one hour.

2. Adsorbent Development

Leaves of *Syzygium cumini* of an indigenous variety were obtained from a local garden. The process of their development as adsorbent was divided into three steps. The first step involved the washing of leaves, first with tap water and then with distilled water to remove the foreign impurities and drying overnight in oven at 85 °C. In the second step, dried leaves were ground to a fine powder using TCEP-FW80 electric grinder at 60 mesh sizes. The obtained powder was further sieved to obtain the exact 60 mesh sized particles. Third step involved the chemical treatment of powder by boiling it with methanol to remove inorganic and organic matter from their surface. The process of boiling and filtration was continued till the filtrate turned colorless. Activation of adsorbent was carried out by finally washing with distilled water and heating it at 85 °C for 15 minutes in an oven, for removal of moisture content. The dried powder of uniform size was placed in a vacuum desiccator to be used as an adsorbent for further studies.

3. Characterization of Adsorbent

The functional groups present in the adsorbent were identified by FTIR spectroscopy using KBr as back ground. The pellets were obtained by pressing a 0.25 g of KBr and 0.004 g of powder adsorbent under a constant pressure of 500 Kg/cm^2. Quantachrome NOVA 2200C USA, surface area analyzer was used for surface area, pore size and pore volume measurements using a mixture of 23% nitrogen and 77% helium. Multipoint BET and Langmuir surface area was determined. Costech Instrument 4010 was used for the elemental analysis of the adsorbent. Hitachi S-3500N scanning electron microscope was used for scanning the adsorbent surface.

4. Batch Adsorption Studies

The adsorption studies of CV and EB onto the leaves of *Syzygium cumini* from aqueous solution were conducted by using the batch equilibrium method. Studies were done in 250 mL glass stoppered, Erlenmeyer flasks using 25 mg L^{-1} of dye concentration with 50 mL of working volume. Initial studies aimed to optimize the adsorption conditions in terms of initial doses of adsorbent (0.1 to 0.8 g), pH of working solution (pH 2 to pH 11), contact time (15 min to 120 min), temperature (298 K to 313 K) and effect of salts on working solution. Optimized amount of adsorbent was added to the solution in each flask which was agitated at a constant speed of 100 rpm for 60 minutes in Brunswick C-24 incubator shaker (New Brunswick Scientific, Canada) at 308±1 K. After a predetermined time interval, required to establish the equilibrium between adsorption and desorption, samples were collected, for their analysis in terms of concentration of dye left in solution after adsorption, which was investigated by measuring its absorbance at appropriate wavelengths corresponding to the maximum absorbance of each dye using UV/VIS spectrophotometer (Hitachi U-100). The amount of dye adsorbed per unit mass of adsorbent (mg/g) was calculated using the equation [19]:

$$q_e=(C_o-C_e)V/m \quad (1)$$

where, C_o and C_e are the initial and residual concentrations of dye in the solution (mg/L), m is the dose of adsorbent (g), and V is working volume (L). The percent removal of dye was calculated in terms of the following equation [20]:

$$\text{Removal of dye (percent)}=\frac{C_o-C_e}{C_o}\times 100 \quad (2)$$

All the experiments were performed in triplicate to ensure the reproducibility of obtaining data. Linear regression analysis of obtained data was performed using Microsoft Excel 2010 program to determine the slope and intercept of the linear plots.

5. Column Studies

Fixed-bed continuous flow column adsorption studies were conducted in a column made of Pyrex glass with inner diameter of

4.5 cm and 25 cm long. At the bottom of the column, a layer of glass wool was placed to prevent loss of adsorbent. The slurry of adsorbent was made and was put into the column leading to the formation of adsorbent bed over the glass wool support. Dye solutions of 30 mg/L and 32 mg/L for CV and EB were then passed through the column with flow rate of 0.5 mL/min, respectively. From the collected volumes of the dyes solutions after a specified time interval, the dye concentration was measured spectrophotometrically till the absorbance of the collected solution matched with that of the fed dye solution.

After the columns were exhausted, a 0.1 M HCl solution was used for desorbing the dye. It was passed through the columns with a constant flow rate 0.5 mL/min. Once complete elution of the dye from the column had taken place, the columns were washed properly with distilled water.

THEORY

1. Adsorption Isotherms

Under isothermal conditions, the relationship between the amount of adsorbate, adsorbed and equilibrium pressure of gas or concentration of solute in solution is termed as adsorption isotherm or adsorption model [21]. The adsorption isotherm is fundamental in describing the behavior between adsorbate and adsorbent and is necessary to ratify the adsorption process [20]. The equilibrium adsorption data are interpreted in terms of different adsorption models. In the present work, equilibrium adsorption data for both dyes was obtained at 308±1 K by adding 0.1 g of adsorbent in 50 ml of dye solution at varying concentration between 20 to 200 mg/L. The obtained data were interpreted in terms of Dubinin-Radushkevich (D-R) [22,23], Freundlich [23,24], Temkin [25,26] and Langmuir [23,27] adsorption models.

$$\text{Dubinin-Radushkevich: } \ln C_{ads} = \ln X_m - \beta\varepsilon^2 \tag{3}$$

where C_{ads} represents the amount of adsorbate up taken by adsorbent (mg/g) and X_m is the maximum adsorption capacity of adsorbent (mg/g), β is constant related to adsorption energy (kJ/mol) [23]. The variable ε is the Polanyi adsorption potential and is given as [23]:

$$\varepsilon = RT\ln\left(1+\frac{1}{C_e}\right) \tag{4}$$

$$\text{Freundlich: } \log C_{ads} = \log C_m + \frac{1}{n}\log C_e \tag{5}$$

Here C_m is the Freundlich constant and is regarded as the multilayer adsorption capacity of adsorbent (mg/g) or degree of adsorption and 1/n is a constant related to adsorption intensity. Its value varies with the degree of heterogeneity and is related to the distribution of bonded ions on the surface of adsorbent. Generally, n>1 is an indication that that adsorbate is much feasibly attached on the surface of adsorbent: the higher the value of n from unity, the higher is the adsorption intensity.

$$\text{Temkin: } q_e = k_1 \ln k_2 + k_1 \ln C_e \tag{6}$$

where k_1 is the Temkin isotherm energy constant (L/mg), and k_2 is the Temkin isotherm constant.

$$\text{Langmuir: } \frac{C_e}{C_{ads}} = \frac{1}{QK_L} + \frac{C_e}{Q} \tag{7}$$

The parameter Q is the maximum adsorption capacity or maximum mass of dye adsorbed (mg/g), and K_L represents the equilibrium constant of adsorption (dm^3/mg), Both Q and K_L are called Langmuir constant and K_L is a temperature dependent parameter. A dimensionless parameter R_L [28] is calculated by using the value of K_L, which indicates the extent of adsorption with change in concentration as:

$$R_L = 1/(1+K_L C_o) \tag{8}$$

$0<R_L<1$ value indicates that adsorption process is favorable, whereas $R_L>1$ exhibits that adsorption process is unfavorable in nature [29].

2. Adsorption Dynamics

Adsorption dynamics involves the characterization of the adsorption process in terms of pseudo-first-order or pseudo-second-order mechanism. The kinetics of adsorption, in the present work, was studied at three different working temperatures (298, 303 and 308 K) by varying the contact time (10 to 60 minutes) and by keeping the initial concentration of both dyes fixed at 25 mg/L. The obtained data were evaluated to check its validity for pseudo-first order or Lagergren equation [30,31] and pseudo-second order rate equations [32,33] as:

$$\text{Pseudo-first order: } \log(q_e - q_t) = \log q_e - \frac{k_1}{2.303}t \tag{9}$$

where k_1 is the rate constant for pseudo-first order kinetics.

$$\text{Pseudo-second order: } \frac{t}{q_t} = \frac{1}{k_2 q_e^2} + \frac{1}{q_e}t \tag{10}$$

Here k_2 indicates the rate constant for pseudo-second order reaction.

Both of these models do not provide the mechanism of mass transport on the surface of adsorbent [20]. A comprehensive model of intraparticle diffusion [34] was also tested to assign the rate controlling step during adsorption of dyes on the surface of adsorbent.

$$\text{Intraparticle diffusion: } q_t = k_t t^{0.5} \tag{11}$$

To demonstrate the particle diffusion kinetics more comprehensively, Boyd, Adamson and Myers equation for the kinetics of particle diffusion [35,36] was used. The amount adsorbed at a particular time was expressed as fraction of the amount adsorbed after infinite time [36] as:

$$F = \frac{Q_t}{Q_\infty} = \frac{\text{amount adsorbed after time t}}{\text{amount adsorbed at Equilibrium (i.e. t = } \infty)} \tag{12}$$

F can be regarded as fractional attainment of equilibrium [35]. Assuming that particle diffusion is a sole rate-controlling process and adsorbent particles are of radius r, it can be expressed as [36]:

$$F = 1 - \frac{6}{\pi^2}\sum_{n=1}^{\infty}\frac{e^{-n^2 B_t}}{n^2} \tag{13}$$

where $B = \pi^2 D_i / r^2$

D_i is the effective diffusion coefficient of adsorbate on the surface of adsorbent. From calculated values of F, tabulated values of B_t can be obtained from Reichenberg table [36]. B_t values are plotted against time and a straight line is obtained having slope a equal to B.

To investigate the main kinetic controlling step between particle diffusion and film diffusion, the applicability of following double logarithmic Bangham's equation [37] was established.

$$\log\log\left(\frac{C_o}{C_o - q_t m}\right) = \log\left(\frac{k' m}{2.3030 V}\right) + \alpha \log t \tag{14}$$

Here α and k′ are constants of Bangham's equation. The constant α is always less than one.

3. Thermodynamic Studies

Activation energy of CV and EB adsorption on *Syzygium cumini* was calculated by the Arrhenius equation [20].

$$\ln k = \ln A - \frac{E_a}{RT} \tag{15}$$

From the slope of the regression line between ln K and 1/T, activation energy Ea (kJ/mol) was calculated. The thermodynamic parameters like, ΔG, ΔH and ΔS were estimated by studying the adsorption process at different temperatures. From the linear plot between ln K_c and 1/T, the values of ΔH and ΔS were estimated using slope and intercept respectively of van't Hoff equation [23,38]:

$$\ln K_c = \frac{-\Delta H}{RT} + \frac{\Delta S}{R} \tag{16}$$

where Langmuir constant $K_c = C_{ads}/C_e$

The value of K_c also provides the magnitude of ΔG by following expression [20]:

$$\Delta G = -RT \ln K_c \tag{17}$$

3. Column Studies

The column efficiency was estimated in terms of various parameters obtained from the breakthrough curves, which are a plot between column effluent concentration versus volume treated or time of treatment. Breakthrough capacity, exhaustion capacity and degree of column utilization are the important features of the breakthrough curves which are estimated from parameters such as length of the primary adsorption zone (δ), total time involved for the establishment of primary adsorption zone (t_x), time for the primary adsorption zone to move down its length (t_δ), time for initial formation of primary adsorption zone (t_f), mass rate flow of the adsorbent (F_m), and fractional capacity of the column (f). The parameters are calculated from the breakthrough curves using following relations [13].

$$t_x = \frac{V_x}{F_m} \tag{18}$$

$$t_\delta = \frac{V_x - V_b}{F_m} \tag{19}$$

$$\frac{\delta}{D} = \frac{t_\delta}{t_x - t_f} = \frac{t_\delta}{t_x + t_\delta(f-1)} = \frac{V_x - V_b}{V_b + f(V_x - V_b)} \tag{20}$$

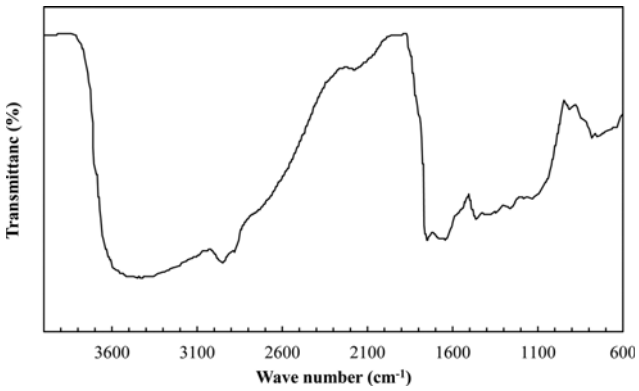

Fig. 1. FTIR spectra of *Syzygium cumini* leaves powder used as adsorbent.

$$f = 1 - \frac{t_f}{t_\delta} = \frac{M_\delta}{(V_x - V_b)C_o} \tag{21}$$

$$\text{Percent saturation} = \frac{D + \delta(f-1)}{D} \times 100 \tag{22}$$

RESULTS AND DISCUSSION

1. Characterization of the Adsorbent

The structural characterization of adsorbent based on the leaves of *Syzygium cumini* has been well described in the literature [39]. It contains OH groups (sharp and broad peak at 3,478 cm^{-1}) (Fig. 1) which are involved in inter- and intramolecular hydrogen bonding and give birth to macromolecular associations like lignin and cellulose. Hydrogen bon2ding is the fundamental characteristic of such macromolecules. The OH groups in *Syzygium cumini* can be present in the form of free hydroxylic groups or in the form of aliphatic carboxylic acids. The presence of aliphatic carboxylic acids is confirmed by its C-H stretching, band at 2,949 cm^{-1} and C=O stretching band at 1,747 cm^{-1}. This band also establishes the presence of esters (-$COOCH_3$) in the leaves of *Syzygium cumini*. Weak band at 1,248 cm^{-1} may be attributed to the bending vibrations of OH groups, which further confirms the presence of alcohols, phenols and carboxylic acids in the adsorbent. In addition, a weak band at 1,129 cm^{-1} indicates the presence of >C=S groups.

The data obtained from elemental, surface area and pore size analysis is shown in Table 2. The data shows a significant percentage of nitrogen and sulfur contents in the adsorbent. SEM image in Fig. 2(a) indicates the mesoporous surface texture of the adsorbent. After adsorption of both CV and EB (Fig. 2(b) and (c)), the regularly spaced conical protrusions and bright spots vanished. This confirms the favored adsorption of both the dyes on mesoporous surface.

2. Optimizations of Adsorption Conditions

Adsorption, being a surface phenomenon, is significantly affected by variations in initial conditions, which imparts physical and chemical changes to both adsorbent and adsorbate. The findings of initial conditions optimizations for adsorption of both CV and EB on *Syzygium cumini* are discussed below.

2-1. Effect of pH

Optimization of pH of adsorption medium is very important

Table 2. Physiochemical characteristics of used adsorbates

Dye	Crystal violet	Eosin B
C.I. number	42555	45400
C.I. name	Basic Violet 3	Acid Red 91
Class	Triarylmethane	Fluorone
Molecular weight (g/mol)	407.99	624.06
Chemical formula	$C_{25}H_{30}ClN_3$	$C_{20}H_6Br_2N_2Na_2O_9$
Water solubility (g/L)	16 (25 °C)	300 (25 °C)
λ_{max}	600 nm (in water)	520 nm (in water)
Synonyms	Basic Violet 3, Gentian Violet	Dibromodinitrofluorescein sodium, Caesar Red
Molecular structure	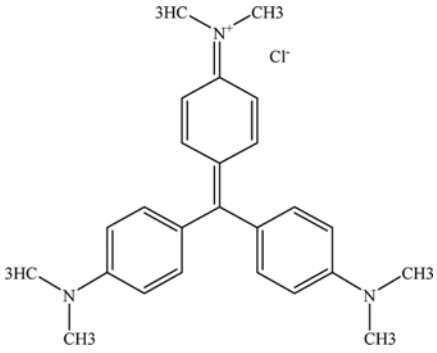	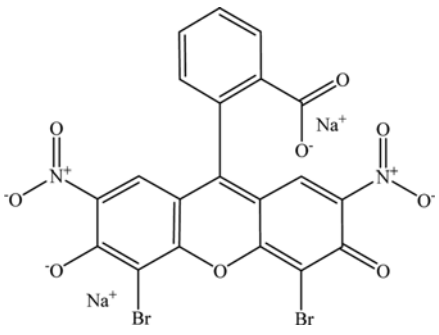

for adsorption studies. Hence, the effect of solution pH on dye removal from solution was studied under identical conditions for both the dyes. As depicted in Fig. 3, both dyes showed opposite behavior towards an increase in pH of adsorption medium. The percentage removal of CV increased precipitously up to pH 4 and then became nearly constant up to pH 12, which is due to the neutralization of the negatively charged surface of adsorbent by positively charged adsorbate molecules. At low pH, the functional groups on the adsorbent surface, which are responsible for adsorption of CV, undergo protonation, so as a result, the surface of the adsorbent becomes positively charged, and this decreases the adsorption of the positively charged CV molecules through electrostatic repulsion. Higher percentage removal of the CV at elevated pH may be attributed to the increased electrostatic interactions between negatively charged adsorption sites on the surface of adsorbent and positively charged nitrogen atom of adsorbate molecules ($=N^+(CH_3)_2$). A similar trend has been reported for removal of CV using Bottom ash, De-oild soya, Grapefruit peel and Wood apple shell [20,40,41]. Basic conditions of adsorption medium favors the removal of CV, hence pH 8 was regarded as optimum pH for further adsorption studies.

The percentage removal of EB decreased from 81% to 60% when the pH of the adsorption medium was increased from 2 to 6 (Fig. 3); however, the further increase in pH did not impart any significant decrease in adsorption and became constant between pH 6 to 12. Minimum percentage removal (55%) was observed at pH 12. This behavior can again be attributed to the influence of pH on the adsorption sites of the adsorbent, the electrostatic forces between adsorbate and these adsorption sites and ionization/dissociation of the adsorbate molecule. Low pH imparts protonation to some groups of cellulose present on adsorbent surface [20] and converts them to $-CH_2-OH_2^+$ and $-OH_2^+$. These protonated groups strongly attract the ph-O^-, and =N-O^- groups on the adsorbate molecules by electrostatic attraction and facilitate the adsorption process. The sharp decrease in percentage adsorption at highly basic conditions may be due to the involvement of electrostatic repulsion between the negatively charged groups on adsorbent surface and the negatively charged EB molecules. The constancy in the removal capacity of *Syzygium cumini* for EB over the pH range 4-12 is an indication that the adsorption process is not solely depending of electrostatic interactions. The possibilities of involvement of hydrogen bonding cannot be ruled out [42]. From these findings, pH 2 was regarded as optimum pH for further adsorption studies of EB.

2-2. Effect of Dose of Adsorbent

Since adsorption capacity is related to the number of adsorption sites, the adsorbent dose is an important parameter that significantly affects the removal of dyes from solution. Study of effect of adsorbent on the removal of CV and EB revealed (Fig. 4) that the adsorption efficiency increased for both dyes as the adsorbent dose was increased from 0.1 to 0.8 g. However, this increase was much sharper for CV as the amount was increased from 0.1 to 0.2 g (from 94.2% to 97.3%), but further increase in amount did not significantly enhance the removal of dye. As reported earlier, the initial rise in percentage removal with adsorbent dose may be due to an increase in the adsorbent surface area and a stronger driving force [40,43] towards adsorption. The constancy in the adsorption of CV after a further increase in adsorbent amount from 0.2 g can be attributed to the saturation of adsorption sites and to the involvement of various types of interactions, like aggregation, between adsorbent particles [44] at enhanced dose. Hence, 0.2 g was considered optimum dose of adsorbent for further CV adsorption studies.

The percentage removal of EB, initially, increased gradually as the dose of adsorbent was increased from 0.1 to 0.6 g (Fig. 4); however, this increase was accelerated by a further increase in the amount

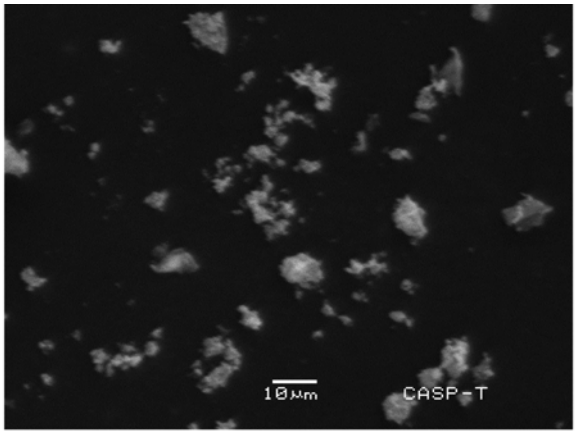

(a)

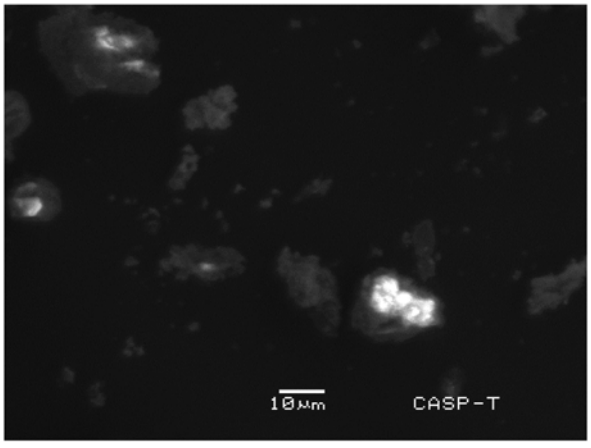

(b)

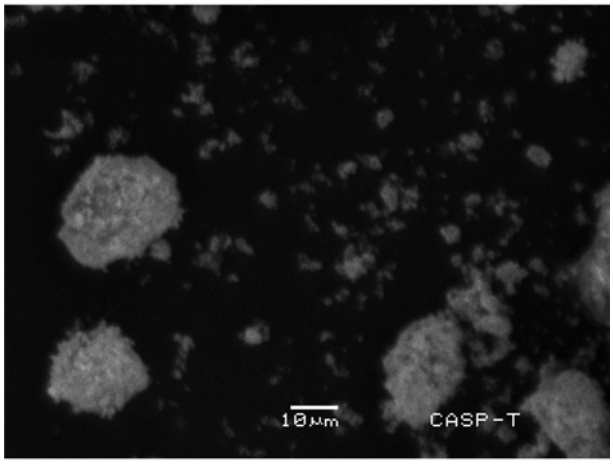

(c)

Fig. 2. Scanning Electron Micrographs of *Syzygium cumini* leaves (a) unabsorbed leaf powder, (b) loaded with CV, (c) loaded with EB.

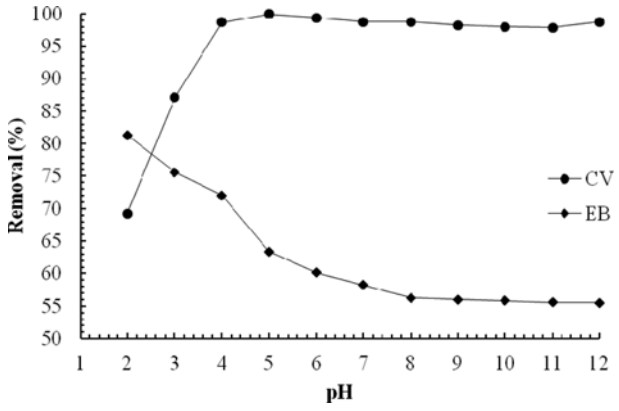

Fig. 3. Effect of pH on percentage removal of CV and EB over *Syzygium cumini* at 308 K.

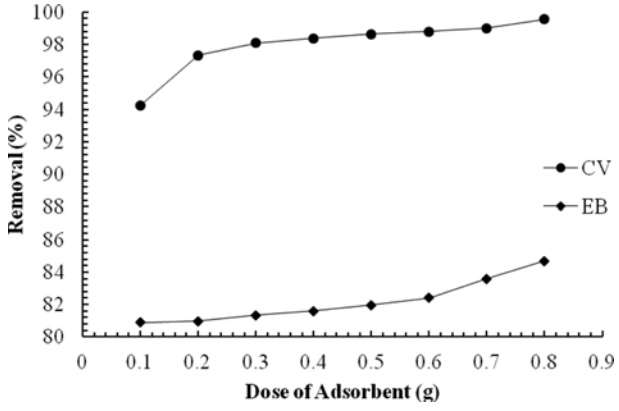

Fig. 4. Effect of dose of adsorbent on percentage removal of CV and EB over *Syzygium cumini* at 308 K (solution pH for CV=8 and for EB=2).

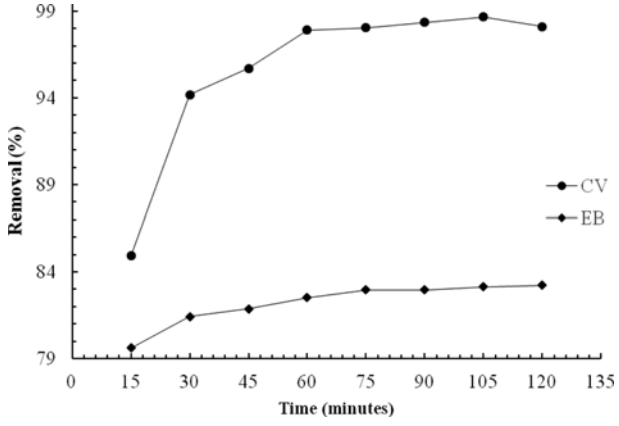

Fig. 5. Effect of contact time on percentage uptake of CV and EB by *Syzygium cumini* at 308 K (Dose of adsorbent=0.2 g for CV and 0.6 g for EB, solution pH=8 for CV and 2 for EB).

of adsorbent, and maximum removal of 84.6% was observed at 0.8 g of adsorbent, which can again be attributed to increase in the surface area of adsorbent with increase in dose that leads towards an increase in the adsorption sites available for EB. It can be concluded that adsorption of EB is not much influenced at the small amount of adsorbent due to multiple reasons like unaltered diffusional path length [45], small particulate aggregation [44] and the nature of adsorbate molecules [42]. Due to the enhanced percentage removal of EB, 0.6 g of adsorbent was regarded as optimum amount of EB

removal studies.

2-3. Effect of Contact Time

Study of contact time gives an indication of the threshold time required to establish the equilibrium between adsorption and desorption. The results of contact time variation for both CV and EB are depicted in Fig. 5. The effect of shaking time is much more conspicuous in case of CV. Percent removal increases from 85 to 98% between the first 15 to 30 minutes of contact time. However, it becomes slow with further increase in contact time, and finally becomes time independent after 60 minutes. Similar behavior has been reported in literature for CV using various adsorbents [19,20,43]. The effect of contact time is not much pronounced for EB (Fig. 5) and equilibrium is visibly attained after 75 minutes of shaking. In both cases, the initial rise in the percentage removal of dyes can be attributed to a number of reasons like large amount of surface area available for adsorption, strong attractive forces between the adsorbate molecules and the adsorption sites of adsorbent, elevated diffusion on the external surface of adsorbent, which leads toward fast pore diffusion into the intra-particle matrix and results in a rapid attainment of equilibrium [46]. The decrease in adsorption in higher contact time gradually leads towards equilibrium. This decrease may be associated with a decrease in the total adsorbent surface area and fewer available binding sites on adsorbent. Hence, from these studies, the equilibrium time for maximum dye uptake was regarded as 60 minutes for CV and 75 minutes for EB.

2-4. Effect of Temperature

Fig. 6 presents the percentage removal of CV and EB as a function of temperature. Both dyes behave differently as the temperature of adsorption system is increased. The percentage removal of CV is augmented from 78.6% to 99.9% as the temperature was increased from ambient to 313 K. This increase was quite drastic between 298 K to 303 K and then became nearly independent of temperature. The increased uptake of CV at higher temperature indicates that adsorption in this system was an endothermic process and leads towards higher surface coverage at elevated temperature. This may be attributed to the increased penetration of CV inside micropores of adsorbent due to reduced solution viscosity at higher temperatures, which also enhances the rate of diffusion of the adsorbate molecules across the external boundary layer or increased interactions between adsorbate molecules and adsorption sites. It is the usual trend for both gasses or liquids that adsorption is exothermic and an increase in temperature abates the adsorption due to release of heat as the result of the development of strong interactions between adsorbate and adsorbent [42,47,48]. The behavior of CV in the present study apparently looks peculiar, but trends similar to this can be seen in literature [49-53].

As depicted in Fig. 6, the rise in temperature decreased the percentage uptake of EB, but this decrease is not much drastic and percentage removal declined only up to 84.7% from 86% as the temperature was increased from 298 K to 313 K. This negligible decline in the removal indicates that adsorption of EB is an exothermic process but it is accompanied with very small heat changes. The decrease in the percentage removal of EB may be attributed to the weakening of the bonds between the EB molecules and the binding sites on the surface of adsorbent and due to favoring of the reverse process (desorption) of exothermic interactions at increased temperature.

2-5. Effect of Initial Concentration

Fig. 7 demonstrates the effect of initial concentration of dyes on their adsorption over *Syzygium cumini*. The percentage removal of both dyes, decreased with increase in initial concentration; however, this decrease is much marked for EB where an increase in the initial concentration up to 120 mg/L resulted in a decline in removal up to 8.5% from 90.4% at the concentration of 20 mg/L. The decrease in the percentage removal for CV is not much significant as compared to that of EB. A gradual 20% decrease in the removal of CV was observed when initial concentration was accreted to 120 mg/L. The decrease in the removal of both dyes by an increment in their concentration can be attributed to the deficiency of sufficient surface area available on adsorbent to accommodate many more molecules of the adsorbate present in the solution. It can be attributed to the fact that lower concentration paves the way for adsorbate molecules in solution to interact with all binding sites on the adsorbent surface and results in a higher percent-

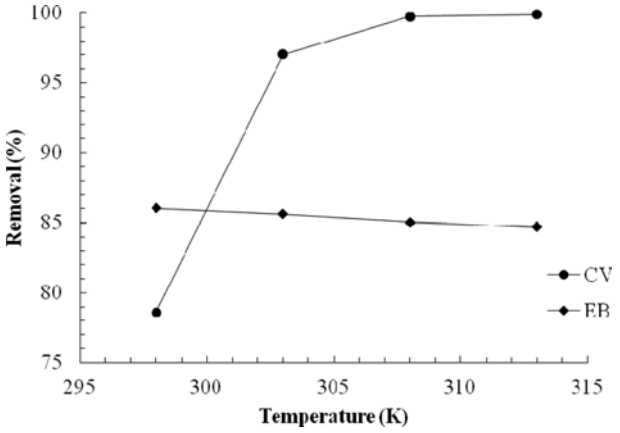

Fig. 6. Effect of temperature on percentage removal of CV and EB over *Syzygium cumini* at contact time of 60 and 75 minutes respectively (Dose of adsorbent=0.2 g for CV and 0.6 g for EB, solution pH=8 for CV and 2 for EB).

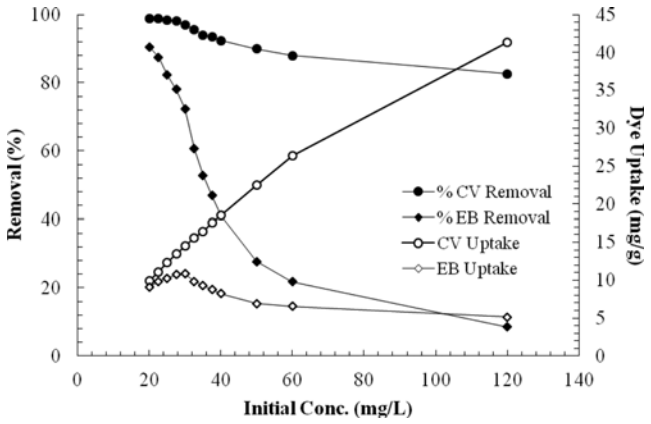

Fig. 7. Effect of initial concentration of CV and EB on their percentage removal and uptake at 308 K and contact time of 60 and 75 minutes, respectively (Dose of adsorbent=0.2 g for CV and 0.6 g for EB, solution pH=8 for CV and 2 for EB).

Table 3. The effect of salts on adsorption of CV and EB using 25 mg/L initial concentration

	KCl	KBr	$AgNO_3$	$CdCl_2$	$HgCl_2$
Dye uptake (mg/g) with salt concentration=0.1 M					
CV*	10.516	12.482	7.771	11.964	12.471
EB**	7.001	6.682	5.915	6.363	7.722
Dye uptake (mg/g) with salt concentration=0.01 M					
CV	11.322	12.342	10.634	12.491	11.431
EB	8.932	9.611	8.127	9.029	7.940

*Normal uptake value for CV without salt=12.30 mg/g
**Normal uptake value for EB without salt=10.28 mg/g

age removal at low concentration. However, all these adsorption sites of adsorbent get saturated at higher concentration of adsorbate and result in a decrease in removal.

Fig. 7 shows that the uptake of CV increased with increase in dye concentration, which is an opposite trend from that of its removal. This increased uptake (9.8-41.3 mg/g) may be attributed to increase in concentration gradient in solution, i.e., increase in the driving forces towards adsorbent and to the involvement of energetically less favorable adsorption sites at increased concentration [26]. The uptake trend of EB was unique: it first increased precipitously as the initial concentration was increased from 20 mg/L to 30 mg/L and then started decreasing with further increase in concentration. The initial increase may again be attributed to the enhanced effect of concentration gradient and large available adsorption sites, but decrease in uptake may be due to increased interactions between adsorbate molecules at increased concentration, which reduces the extent of adsorption.

2-6. Effect of Salts

The presence of salts in adsorption system affects the removal of dye due to the formation of their interactions with adsorbate and adsorbent [54]. Table 3 indicates that uptake of CV increases from its normal value on the additions of salts like KBr and $HgCl_2$. However, the addition of $AgNO_3$ imparts a slight reduction in its uptake when concentration of this salt is higher. Under dilute condition, $CdCl_2$ enhances the uptake from its normal value. The change in uptake of CV is less obvious when KCl is used. The addition of salts in the adsorption system of EB reduces its uptake both under low or high dilutions of salts. However, the effect of higher concentration is more obvious in terms of reduction. The effect of those salts which increase the dye uptake can be explained in terms of their neutralization of negatively charged parts of adsorbate molecules and the negatively charged surface of adsorbent and reduce the electrostatic repulsion on both ends [54]. The electrostatic repulsions between the adsorption sites and adsorbate molecules is such influencing in the micropores. The diffusion of adsorbate molecules into these micropores is hindered by the negatively charged surface of adsorbent. The addition of salts in such systems screened this repulsion and enhanced the dye uptake. Similarly, some of these salts can also work to neutralize the positively charged surface of adsorbent and diminish the electrostatic attractions between dye molecules and adsorption sites. The counterions of salts also compete with negatively charged adsorbate molecules for the single adsorption site and reduce the dye uptake. This reduction in dye uptake by the addition of salts signifies that various types of interactions, other than electrostatic interactions between adsorbate and adsorbent, are also involved in the adsorption process. In addition, the effect of the ionic strength on the adsorption process of dyes has been well established [55-57]. The increased ionic strength of the adsorption system usually increases the dye uptake by enhancing the aggregation of dye molecules and improving the electrostatic attractions.

3. Adsorption Isotherms

The magnitudes of constants obtained from the plots of D-R ($\ln C_{ads}$ versus ε^2), Freundlich ($\log C_{ads}$ versus $\log C_e$), Langmuir (C_e/C_{ads} versus C_e) and Temkin (q_e versus $\ln C_e$), for adsorption of both CV and EB over Syzygium cumini are listed in Table 3. The plots of adsorption isotherm data with correlation coefficients of linear regression are shown in Figs. 8, 9, 10 and 11, respectively.

The correlation coefficients for both CV and EB indicate that the equilibrium data is fitted well to D-R isotherm for CV, but it is poorly modeled for EB. The constant β of D-R isotherm can be used to calculate the mean free energy of adsorption (E) by the following relationship [58]:

$$E = \frac{1}{\sqrt{2\beta}} \tag{18}$$

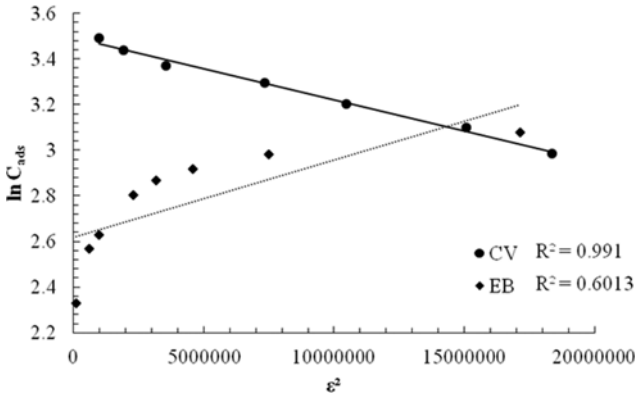

Fig. 8. D-R adsorption isotherm for adsorption of CV and EB over *Syzygium cumini* ($\varepsilon^2 \times 200$ was plotted for EB).

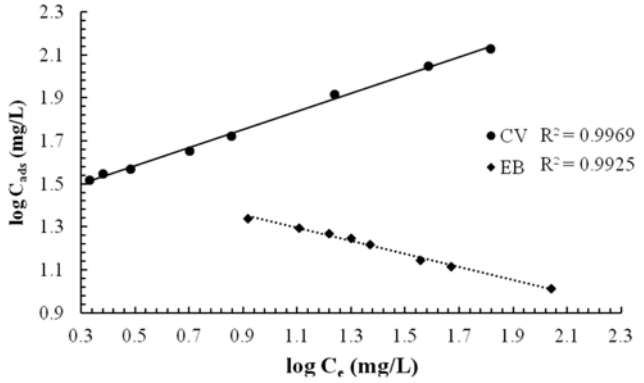

Fig. 9. Freundlich adsorption isotherm for adsorption of CV and EB over *Syzygium cumini*.

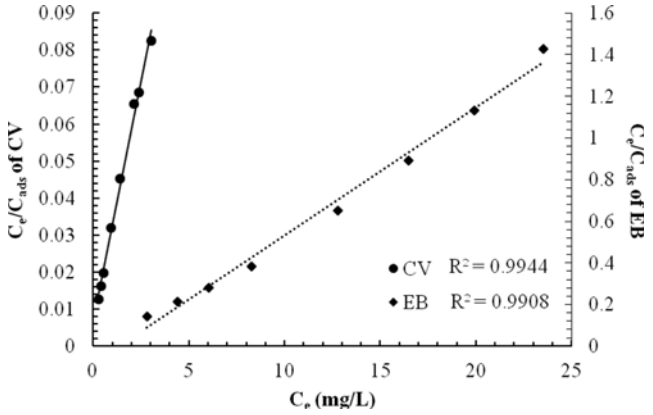

Fig. 10. Langmuir adsorption isotherm for adsorption of CV and EB over *Syzygium cumini*.

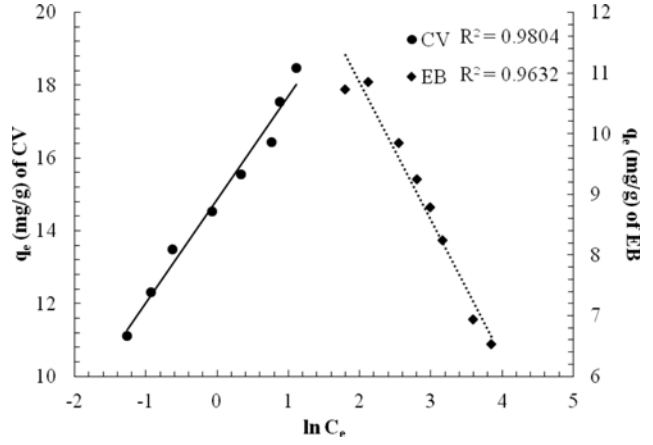

Fig. 11. Temkin adsorption isotherm for adsorption of CV and EB over *Syzygium cumini*.

The value of energy calculated using the above equation provides an idea about the type and nature of adsorption process. The process may be regarded as physisorption (physical adsorption) if the magnitude of E is less than 8 kJ mol^{-1} and it becomes a chemical ion exchange process if E is between 8 to 16 kJ mol^{-1} [58]. The value of energy was calculated as 4.081 kJ mol^{-1} for CV and 0.267 kJ mol^{-1} for EB. It implies that the adsorption of EB is a physical adsorption process involving weak van der Waals forces. The higher value of energy for CV indicates that it is more strongly attached on the surface of adsorbent than EB. Fig. 9 shows that both CV and EB are strongly following the logarithmic model of the Freundlich isotherm but with opposite trend. The Freundlich model exhibits a slightly better fit to the adsorption data than the D-R model for CV, but the almost unity value of correlation coefficient for EB indicates that the results are significantly better and experimental data are strongly fitting this model than D-R model of the isotherm. The magnitude of heterogeneity factor or adsorption intensity, i.e., n for both the dyes (Table 4), illustrates that adsorbates are favorably adsorbed on the adsorbent, and higher value of n for CV indicates its higher adsorption intensity than EB.

The correlation of adsorption data of both CV and EB was extremely high with theoretical model for monolayer adsorption, i.e., Langmuir isotherm model with R^2 values nearly unity for both systems (Fig. 10). The maximum adsorption capacity of *Syzygium cumini* for CV and EB, calculated from the regression analysis of Langmuir isotherm data is 38.750 and 16.286 mg/g (Table 4), respectively, at 308 K. The values of dimensionless equilibrium separation factor R_L calculated using Langmuir constant are between 0.236 to 0.051 for CV and 0.0569 to 0.032 for EB, clearly indicating the favorability of adsorption of both dyes. The lower value of R_L for CV at higher concentration indicates that adsorption is more favorable at high concentration of dye. The validity of the Langmuir isotherm further establishes that adsorption of dyes is accompanied with monolayer formation. It is well established in the literature [59] that the dye molecules adsorbed favorably on adsorbent with low competition of solvent molecules, and the surface of adsorbent gets saturated slowly with dye molecules until the concentration reaches its maximum value (Q). In addition, the process of multilayer formation is less favorable due to the presence of electrostatic repulsion between adsorbed molecules and those finding the adsorption sites [60]. The plot of equilibrium adsorption data for validity of Temkin isotherm indicates that both CV and EB follow this isothermal model of adsorption, but like Freundlich and D-R models the trend of fitting for both dyes is opposite. The calculated values of Temkin isotherm energy constant and Temkin constant are given in Table 4. As indicated by R^2 values (Fig. 11), the validity of the Temkin model of adsorption is less both for CV and EB than Langmuir and Freundlich models, but for EB it is much better fitted

Table 4. D-R, Langmuir, Freundlich and Temkin constants for adsorption of CV and EB over *Syzygium cumini*

Dye	D-R constants		Langmuir constants		Freundlich constants		Temkin constants	
	X_m (mg/g)	β ($mmol^2/J^2$)	Q (mg/g)	K_L	C_m (mg/g)	n	k_1 (L/mg)	k_2
CV	32.890	3×10^{-8}	38.750	3.739	23.520	0.422	2.848	1.83×10^{2}
EB	13.610	7×10^{-6}	16.286	0.735	42.360	0.302	2.268	8.78×10^{2}

Table 5. Kinetic parameters for adsorption of CV and EB over *Syzygium cumini*

Dye	$q_{e,exp}$ (mg/g)	Pseudo-first order kinetic model		Pseudo-second order kinetic model	
		$q_{e,calc}$ (mg/g)	k_1 (min^{-1})	$q_{e,calc}$ (mg/g)	k_2 (g/mg min)
CV	49.787	27.797	0.118	51.020	0.014
EB	10.288	10.431	0.068	11.876	0.008

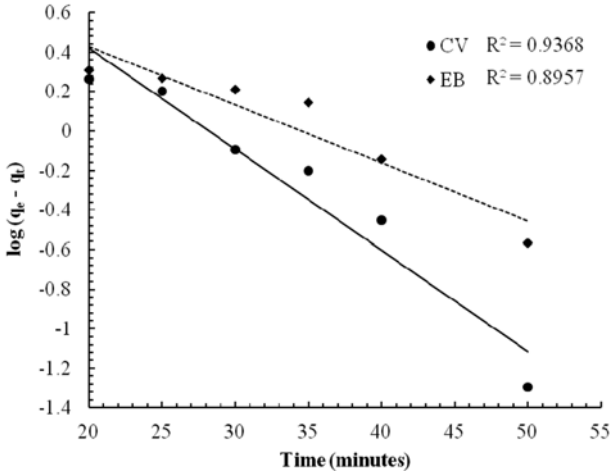

Fig. 12. Lagergren's plot for adsorption of CV and EB over *Syzygium cumini*.

than D-R isotherm.

4. Adsorption Dynamics

The values of the pseudo-first order rate constants, k_1 and equilibrium adsorption capacity q_e (Table 5) calculated from the slopes and intercepts, respectively, of the Lagergren plots for pseudo-first order kinetics (Fig. 12), provide that calculated and experimental equilibrium adsorption capacity q_e, differs widely for CV but is in agreement for EB. The correlation coefficients for both dyes, which are the sole measure of validity of this kinetic model, are significantly lower from unity. It can be attributed from these findings that the adsorption kinetics of CV and EB on *Syzygium cumini* cannot be established using Lagergren's model. The variations in experimental results from Lagergren's plot are not solely due to the nature of this adsorption process but may also be attributed to certain shortcomings associated with this mathematical expression [61]. It is considered that variables along ordinate, i.e., log $(q_e - q_t)$ represent the number of available sites, which, in actuality varies largely from consideration [61]. The equilibrium adsorption capacity q_e, calculated from intercept of this expression is an adjustable parameter, usually found to be not representing the parameter obtained from the intercept of actual pseudo-first-order plot. In addition, it has been established that Lagergren's equation is generally applicable over the initials of adsorption process between 20 to 30 minutes [62]. Conversely, the kinetic data of both CV and EB exhibited an excellent compliance with pseudo-second-order kinetic model. The plot of t/q_t against t showed excellent linearity (Fig. 13) with a correlation coefficient of unity for CV and close to unity for EB. As shown in Table 5, the calculated q_e values using this kinetic model, agree with experimental q_e values for both adsorbate systems. The excellent correlation for both the systems indicates that the adsorption process is following the pseudo-second-order kinetics, which establishes that the adsorption process involves valence forces by multiple processes like sharing or exchange of electrostatic potential between adsorbent and adsorbate, and the whole adsorption process is comprised of such valence phenomena and transport processes on the surface and any of these can be rate determining. The transport processes on the surface are diffusional processes, such as surface diffusion or bulk penetration, which involves the electrostatic interactions or chemical bond formation along the diffusion path [61]. The intraparticle diffusion model was applied to investigate its possibility as a rate determining process. According to this model, a plot of q_t versus $t^{0.5}$ should be a straight line passing through origin if the adsorption process is being controlled by intraparticle diffusion [63]; however, variation in linearity indicates that the process is being governed by two or more steps. The correlation coefficients in Fig. 13 exhibit that plots for both CV and EB are not exactly linear, which provides that intraparticle diffusion is associated with two other activated diffusional processes, external surface adsorption or film diffusion in which transport of adsorbate to the surface of adsorbent occurs through solution and adsorption of the adsorbate in the interior of the adsorbent. The former can be regarded as initial stages or beginning of adsorption and the latter as the final equilibrium stage. The intraparticle diffusion is an intermediate of these two processes. In addition, as Table 4 indicates for pseudo-second order kinetics, the adsorption process at the adsorbent of both dyes is not rapid, hence accord-

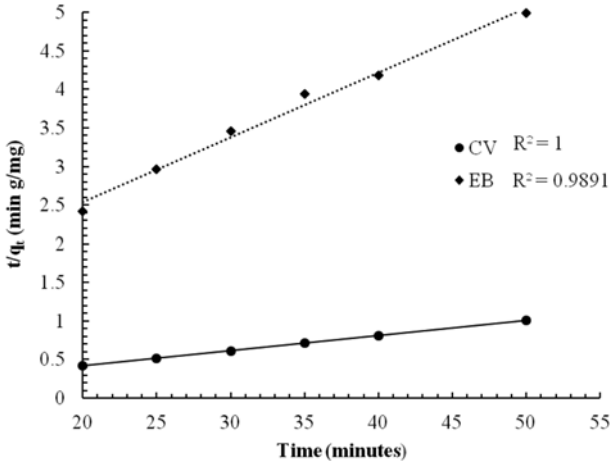

Fig. 13. Plot for validation of pseudo-second order kinetics for adsorption of CV and EB over *Syzygium cumini*.

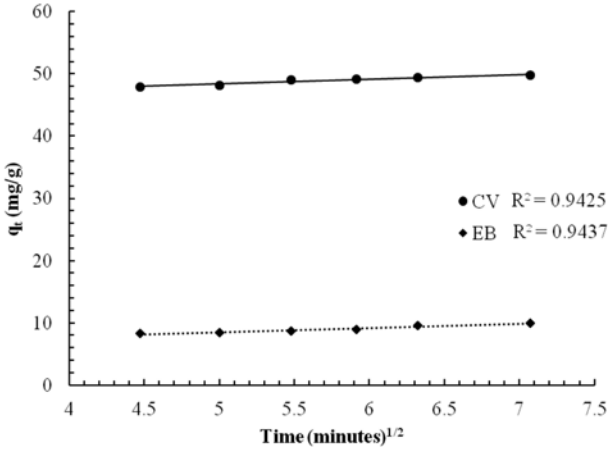

Fig. 14. Validation of Morris-Weber equation for adsorption of CV and EB over *Syzygium cumini*.

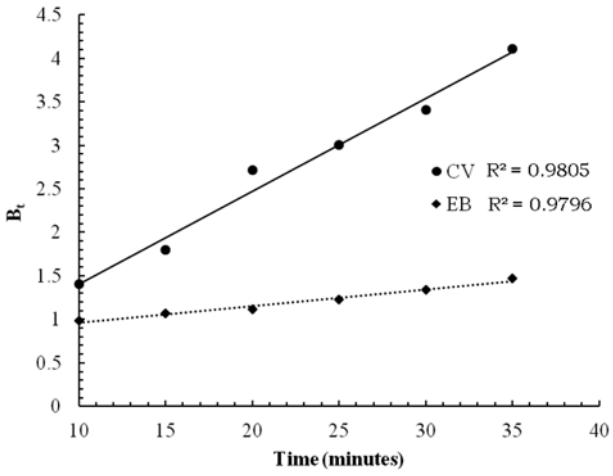

Fig. 15. Validation of Boyd, Adamson and Myers equation for adsorption of CV and EB over *Syzygium cumini*.

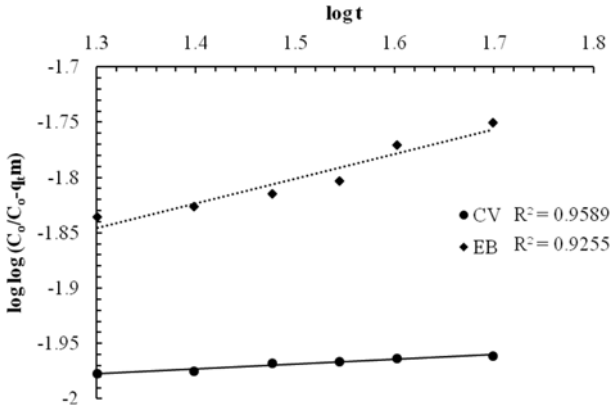

Fig. 16. Bangham plot of CV and EB over *Syzygium cumini*.

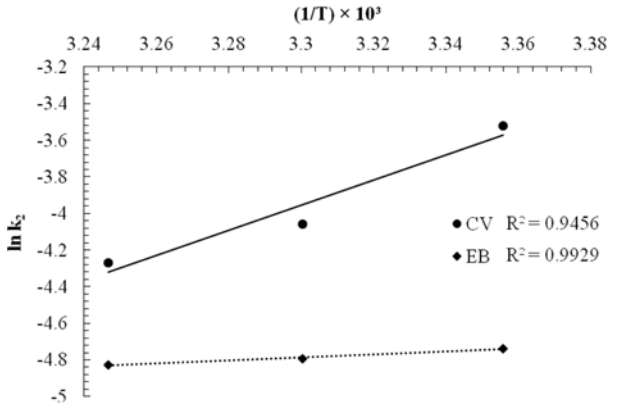

Fig. 17. Arrhenius plot for the determination of activation energy for adsorption of CV and EB on *Syzygium cumini*.

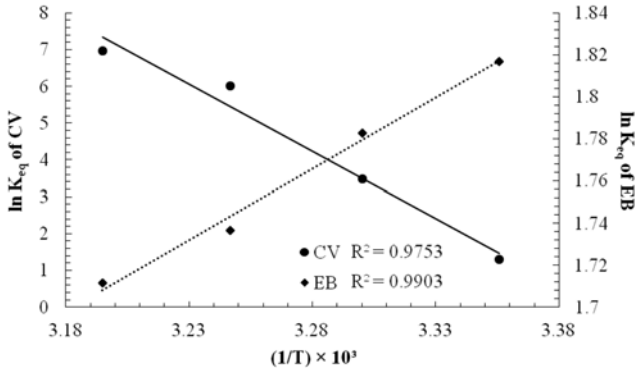

Fig. 18. Variation in adsorption equilibrium of CV and EB on *Syzygium cumini* with temperature.

ing to Aharoni and Sparks [61] these are associated with surface transport processes, i.e., diffusion which also controls the overall rate of adsorption. To distinguish between the significance of film diffusion and particle diffusion adsorption processes for both CV and EB systems, B_t (values obtained from Reichenberg table using calculated fractional attainment F values) versus time graph was plotted (Fig. 15). Straight lines for both the systems which are not passing through the origin suggest that film diffusion is a rate determining process during the adsorption of both CV and EB. Here, external transport of ingoing dye molecules is much greater than the transport of already adsorbed molecules [35,36] into the pores of adsorbent. To validate these findings, Bangham's equation was applied to experimental data. The linearity of this equation indicates that the rate determining step is particle diffusion [63]. But correlation coefficients of plots in Fig. 16 indicate that Bangham's equation for both adsorbates is not exactly linear. Hence, the possibility of particle diffusion as a sole rate controlling process for both EB and CV systems is ruled out, which further strengthens the above findings regarding film diffusion as rate controlling phenomenon.

5. Activation Energy and Thermodynamic Parameters

Using rate constants of pseudo-second order kinetic model at three different temperatures (298 K, 303 K and 308 K), activation energy (E_a) for adsorption of both CV and EB was calculated. From the slopes of Arrhenius plots, i.e., ln k_2 versus 1/T (Fig. 18), activation energy was estimated to be 57.265 and 6.721 kJ/mol for CV and EB, respectively. The magnitude of energy of activation can be used to ratify the nature of the adsorption process. If activation energy is less than 40 kJ/mol, it is classified as physical adsorption, while E_a values higher than this threshold limit can be regarded as chemical adsorption [20]. The magnitude of E_a for CV indicates that the adsorption process is chemical. This higher value of E_a for CV is in agreement with a reported value in literature [20]. While the adsorption of EB can be classified as physical adsorption due to its extremely low magnitude. The values of ΔH and ΔS for both adsorbates were determined from the slope and intercept of the van't Hoff plot (Fig. 17). The values of ΔH for CV and EB were found to be 85.734 and −5.617 kJ/mol, respectively. The positive value of ΔH for CV indicates that the adsorption process is endothermic, whereas a negative value for EB establishes the exothermic nature of adsorption process. The magnitude of ΔH for both systems validates the finding that adsorption of CV on Syzygium cumini is chemisorption, while it is physisorption in case of EB. The values of ΔS were calculated as 102.914 kJ/mol for CV and −3.745 kJ/mol for EB. The positive value of ΔS for CV indicates that its adsorption is associated with significant internal changes in Syzygium cumini, while the negative magnitude of ΔS for EB provides that

Table 6. Magnitude of Gibbs free energy calculated at different temperature for adsorption of CV and EB over *Syzygium cumini*

Temperature (K)	ΔG (kJ/mol) for CV	ΔG (kJ/mol) for EB
298	−3.226	−4.501
303	−8.783	−4.490
308	−15.378	−4.447
313	−18.118	−4.453

though its adsorption is not associated with internal changes in adsorbent but the process is enthalpy driven in nature. Table 6 provides the values of Gibb's free energy (ΔG) both for CV and EB at different temperatures. The negative value of ΔG for both dyes at all temperatures indicates the spontaneous nature of adsorption process. Higher values of ΔG at low temperature indicate that elevated temperature facilitates the adsorption of the CV but reverse response is indicated for adsorption of EB. Hence adsorption is relatively easier for EB at low temperature.

6. Column Studies

It was calculated from the breakthrough curve that 17.45 mg of CV and 12.7 mg of EB were adsorbing over 1 g of adsorbent, respectively. The breakthrough capacity of both the dyes is less than the batch capacity; this may be due to lesser contact time of the dyes with adsorbent which require longer time for equilibration, thus inhibiting the utilization of column capacity. The total time involved for the establishment of primary adsorption zone (t_x), for the CV and EB system, was 3653846.15 and 730769.23 min, respectively, whereas the values for the primary adsorption zone to move down its length (t_δ) were 1000000 and 653846.15 min, respectively (Fig. 19). On comparing the two, it has been noted that the values for the CV system are much higher than EB system. The time for initial formation of primary adsorption zone (t_f) was found to be 5.75 h

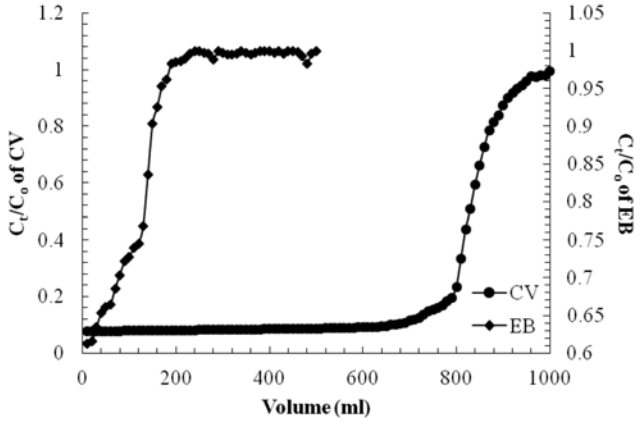

Fig. 19. Breakthrough curve for CV and EB for *Syzygium cumini* column.

Table 7. Fixed bed adsorber calculations

Dye	C_o (mg/L)	C_x (mg/L)	C_b (mg/L)	$V_x - V_b$ (ml)	F_m (mg/cm^2/min)	D (cm)
CV	30	28.73	3.23	260	0.00026	4
EB	32	30.95	19.39	170	0.00026	4

Table 8. Parameters for fixed bed adsorber

Dye	t_x (min)	t_δ (min)	t_f (min)	f (ml)	δ (cm)	% Saturation
CV	3653846.15	1,000,000	345	0.999	1.0948	99.97
EB	730769.23	653846.15	10	0.984	3.5789	99.91

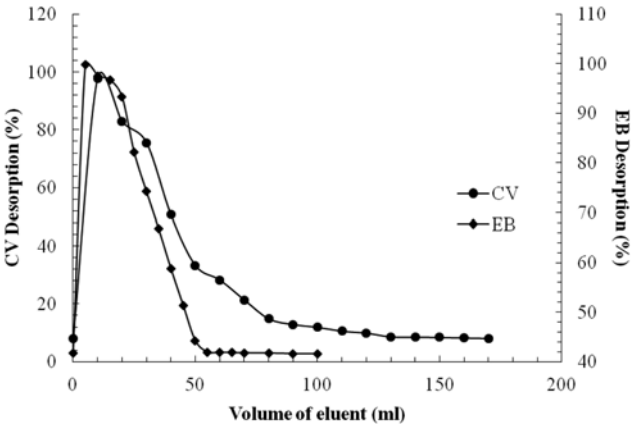

Fig. 20. Desorption of CV and EB from *Syzygium cumini* column.

for CV and 0.17 h for EB, respectively. The values calculated for all the breakthrough parameters are summarized in Tables 7 and 8. The percentage saturation of the column was found to be 99.97% for CV and 99.91% for EB.

Fig. 20 demonstrates desorption curves for both CV and EB. For complete desorption of CV, 170 mL of acidic water was required and for EB, about 55 mL of the eluent brought complete desorption. The percentage recovery of CV and EB was almost 91.94% and 58.08%, respectively. The graphs reveal that out of an adsorbed 3.49 mg of CV, 3.20 mg was removed in total 170 mL of the eluent. On the other hand, an initial 55 mL of eluent desorbed 4.42 mg out of 7.62 mg of total adsorbed EB in the case of column regeneration.

7. Adsorption Mechanism

It can be proposed that adsorption of CV and EB is associated with the presence of alcoholic and carboxylic acidic groups, which provides the platform for adsorption by establishing hydrogen bonding and electrostatic interactions. In aqueous medium, the adsorption of CV is mainly controlled by OH groups, which undergo dissociation to generate -O^- group. This generated anion interacts with cationic CV molecules by strong chemical forces (as indicated by thermodynamic studies) and removes it from aqueous medium. Therefore, elevated pH enhances the rate of CV removal. The process which can also be called as hydrogen-CV ion-exchange can be described as:

Syzygium cumini-OH $\rightleftharpoons$ *Syzygium cumini*-O^- + H^+

Syzygium cumini-O^- + CV^+ $\rightleftharpoons$ *Syzygium cumini*-O-CV

The adsorption process of EB is strongly controlled by the pH of the medium. At low pH, OH groups on the surface of adsorbent undergo protonation and promote the hydrogen bonding between protonated groups on the surface and nitrogen atoms of EB molecule. Lower pH enhances the protonation which in turn increases

the adsorption process. The process can be shown as:

$$\textit{Syzygium cumini}\text{-OH}+H^{+} \rightleftharpoons \textit{Syzygium cumini}\text{-}OH_2^{+}$$

$$\textit{Syzygium cumini}\text{-}OH_2^{+}+O_2N\text{-EB} \rightleftharpoons \textit{Syzygium cumini}\text{-}OH_2^{+}\text{--- }O_2N\text{-EB}$$

From kinetic and surface transport studies, these interactions between adsorbent and dyes can be the first step of the adsorption process where dye molecules interact with the surface from the bulk of aqueous solution. This step is followed by film diffusion or transport of adsorbed dye molecules from the boundary layer to the interior of adsorbent. This step is very significant in the overall adsorption of both dyes, as it has been classified as a rate-controlling step. The last step, which propagates along with the second step until equilibrium is established, is the intra-particle diffusion where dye molecules diffuse into the pores of adsorbent.

CONCLUSION

We investigated the potential use of *Syzygium cumini* leaves as an adsorbent for the aqueous removal of CV and EB. pH 8, 0.2 g of adsorbent and 60 minutes contact time were found to be optimum parameters for effective removal of CV, while maximum removal of EB was observed at pH 2, 0.6 g of adsorbent, and 75 minutes of contact time. High temperature favored the CV adsorption, but the opposite trend was observed for the removal of EB. Presence of salts in the adsorption medium was found to have a profound effect on the adsorption capacity of both dyes. Under optimized conditions both EB and CV strongly followed the Langmuir, Freundlich and Temkin models of adsorption, but variations were observed from D-R adsorption isotherm. Detailed study of adsorption kinetics revealed that the pseudo-second order model is the characteristic of both dyes, and film diffusion was found to be rate controlling step instead of particle diffusion. The adsorption of CV was found to be chemisorption and endothermic, while process was found to be exothermic for EB systems which involves physical interactions with adsorbent but adsorption of both dyes was a spontaneous process and this was inferred from thermodynamic calculations. From the column studies the percentage saturation is found to be 99.97% for CV and 99.91% for EB. Taking into account all the aforementioned studies, it can be concluded that *Syzygium cumini* is an effective, efficient and economic adsorbent for the removal of CV and EB from aqueous medium.

REFERENCES

1. T. Puzyn, *Organic pollutants ten years after the stockholm convention - environmental and analytical update*, InTech, Rijeka (2012).
2. T. Robinson, G. McMullan, R. Marchant and P. Nigam, *Bioresour. Technol.*, **77**, 247 (2001).
3. M. A. Mottaleb and D. Littlejohn, *Anal. Sci.*, **17**, 429 (2001).
4. A. Baban, A. Yediler and N. K. Ciliz, *Clean: Soil, Air, Water*, **38**, 84 (2010).
5. S. Wang, Y. Boyjoo, A. Choueib and Z. H. Zhu, *Water Res.*, **39**, 129 (2005).
6. O. J. Hao, H. Kim and P.-C. Chiang, *Crit. Rev. Env. Sci. Technol.*, **30**, 449 (2000).
7. N. Willmott, J. Guthrie and G. Nelson, *J. Soc. Dyers Colour.*, **114**, 38 (1998).
8. M. Rafatullah, O. Sulaiman, R. Hashim and A. Ahmad, *J. Hazard. Mater.*, **177**, 70 (2010).
9. C. R. Silva, T. F. Gomes, G. C. R. M. Andrade, S. H. Monteiro, A. C. R. Dias, E. A. G. Zagatto and V. L. Tornisielo, *J. Agric. Food Chem.*, **61**, 2358 (2013).
10. C. G. Rocha, D. A. M. Zaia, R. V. d. S. Alfaya and A. A. d. S. Alfaya, *J. Hazard. Mater.*, **166**, 383 (2009).
11. M. Arami, N. Y. Limaee, N. M. Mahmoodi and N. S. Tabrizi, *J. Colloid Interface Sci.*, **288**, 371 (2005).
12. E. Rubin, P. Rodriguez, R. Herrero, J. Cremades, I. Barbara and M. E. Sastre de Vicente, *J. Chem. Technol. Biotechnol.*, **80**, 291 (2005).
13. N. S. Maurya, A. K. Mittal, P. Cornel and E. Rother, *Bioresour. Technol.*, **97**, 512 (2006).
14. K. S. Low, C. K. Lee and L. L. Heng, *Environ. Technol.*, **15**, 115 (1994).
15. Y. S. Ho, D. A. J. Wase and C. F. Forster, *Environ. Technol.*, **17**, 71 (1996).
16. W. Zou, H. Bai, S. Gao and K. Li, *Korean J. Chem. Eng.*, **30**, 111 (2013).
17. G. Mishra and M. A. Tripathy, *Colourage*, **40**, 35 (1993).
18. C. Moran, M. E. Hall and R. Howell, *J. Soc. Dyers Colour.*, **113**, 272 (1997).
19. F. Akbal, *J. Colloid Interface Sci.*, **286**, 455 (2005).
20. S. Chakraborty, S. Chowdhury and P. Das Saha, *Carbohydr. Polym.*, **86**, 1533 (2011).
21. K. J. Laidler, *Chemical kinetics*, Harper & Row, New York (1987).
22. M. M. Dubinin and L. V. Radushkevich, *Chem. Zentr*, **1**, 875 (1947).
23. M. Akhtar, M. I. Bhanger, S. Iqbal and S. M. Hasany, *J. Hazard. Mater.*, **128**, 44 (2006).
24. H. M. F. Freundlich, *J. Phys. Chem.*, **57**, 385 (1906).
25. M. I. Temkin and V. Pyzhev, *Acta Physiochem (URSS)*, **12**, 327 (1940).
26. A. Buasri, N. Chaiyut, K. Tapang, S. Jaroensin and S. Panphrom, *Int. J. Env. Sci. Dev.*, **3**, 10 (2012).
27. I. Langmuir, *J. Am. Chem. Soc.*, **38**, 2221 (1916).
28. G. McKay, H. S. Blair and J. R. Gardner, *J. Appl. Polym. Sci.*, **29**, 1499 (1984).
29. Z. Zawani, A. L. Chuah and T. S. Y. Choong, *Eur. J. Sci. Res.*, **37**, 63 (2009).
30. S. Lagergren, *K. Svenska Vetenskapsakad. Handl.*, **24**, 1 (1898).
31. M. A. Abd El-Ghaffar, M. H. Mohamed and K. Z. Elwakeel, *Chem. Eng. J.*, **151**, 30 (2009).
32. Y. S. Ho and G. McKay, *Process Biochem. (Amsterdam, Neth.)*, **34**, 451 (1999).
33. F.-C. Wu, R.-L. Tseng, S.-C. Huang and R.-S. Juang, *Chem. Eng. J.*, **151**, 1 (2009).
34. W. J. Weber and J. C. Morris, *J. Sanit. Eng. Div. ASCE*, **89**, 31 (1963).
35. G. E. Boyd, A. W. Adamson and L. S. Myers, *J. Am. Chem. Soc.*, **69**, 2836 (1947).
36. D. Reichenberg, *J. Am. Chem. Soc.*, **75**, 589 (1953).
37. D. H. Bangham and F. P. Burt, *Proc. R. Soc. A.*, **105**, 481 (1924).
38. M. Mufazzal Saeed, S. Moosa Hasany and M. Ahmed, *Talanta*, **50**, 625 (1999).
39. K. Rao, S. Anand and P. Venkateswarlu, *Korean J. Chem. Eng.*, **27**, 1547 (2010).
40. A. Saeed, M. Sharif and M. Iqbal, *J. Hazard. Mater.*, **179**, 564 (2010).

41. S. Jain and R. V. Jayaram, *Desalination*, **250**, 921 (2010).
42. D. M. Ruthven, *Principles of Adsorption and Adsorption Processes*, Wiley, New York (1984).
43. R. Ahmad, *J. Hazard. Mater.*, **171**, 767 (2009).
44. O. Aksakal and H. Ucun, *J. Hazard. Mater.*, **181**, 666 (2010).
45. G. Crini, H. N. Peindy, F. Gimbert and C. Robert, *Sep. Purif. Technol.*, **53**, 97 (2007).
46. Y. S. Ho and C. C. Chiang, *Adsorption*, **7**, 139 (2001).
47. J. Mattson and H. Mark, *Activated carbon: Surface chemistry and adsorption from solution*, Marcel Dekker, Inc., New York (1971).
48. S. Faust and O. Aly, *Adsorption processes for water treatment*, Butterworth Publishers, Stoneham (1987).
49. S. Netpradit, P. Thiravetyan and S. Towprayoon, *J. Colloid Interface Sci.*, **270**, 255 (2004).
50. R. F. P. M. Moreira, N. C. Kuhnen and M. G. Peruch, *Latin. Am. Appl. Res.*, **28**, 37 (1998).
51. S. Patil, V. Deshmukh, S. Renukdas and N. Patel, *Int. J. Env. Sci.*, **1**, 1116 (2011).
52. C. Namasivayam and D. Kavitha, *Dyes Pigm.*, **54**, 47 (2002).
53. Y. Guo, J. Zhao, H. Zhang, S. Yang, J. Qi, Z. Wang and H. Xu, *Dyes Pigm.*, **66**, 123 (2005).
54. A. W. M. Ip, J. P. Barford and G. McKay, *J. Colloid Interface Sci.*, **337**, 32 (2009).
55. Y. Hu, T. Guo, X. Ye, Q. Li, M. Guo, H. Liu and Z. Wu, *Chem. Eng. J.*, **228**, 392 (2013).
56. M. Alkan, Ö. Demirbaş and M. Doğan, *Fresenius Environ. Bull.*, **13**, 1112 (2004).
57. L. A. Sepulveda and C. C. Santana, *Environ. Technol.*, **34**, 967 (2012).
58. S. Chowdhury and P. Saha, *Carbohydr. Polym.*, **86**, 1533 (2011).
59. Y. S. Al-Degs, M. I. El-Barghouthi, A. H. El-Sheikh and G. M. Walker, *Dyes Pigm.*, **77**, 16 (2008).
60. C. H. Giles, D. Smith and A. Huitson, *J. Colloid Interface Sci.*, **47**, 755 (1974).
61. C. Aharoni and D. L. Sparks, *Kinetics of Soil Chemical Reactions—A Theoretical Treatment*, Rates of Soil Chemical Processes, Sssaspecialpubl, 1 (1991).
62. P. King, N. Rakesh, S. Beenalahari, Y. Prasanna Kumar and V. S. R. K. Prasad, *J. Hazard. Mater.*, **142**, 340 (2007).
63. E. Tütem, R. Apak and Ç. F. Ünal, *Water Res.*, **32**, 2315 (1998).